Validating the performance of a Raman laser spectrometer (RLS) instrument under Martian conditions

Motamedi Mohammadabadi, K.

2013

document version
Publisher's PDF, also known as Version of record

Chapter 4: The effect of ambient temperature and composition on the Raman study of olivine: implications for the stoichiometric changes

This chapter is the basis of a manuscript that will be submitted to the journal of Raman spectroscopy.

K. Motamedi, A. Colin, J.H. Hooijschuur, G.R. Davies.

Contents

4.1 Introduction

To better determine the mineralogy of other planets we need to fully understand the crystal structure of all minerals so as to predict the signatures obtained by spectroscopic instruments utilised on space missions. Olivine is the common name for a suite of iron-magnesium silicate minerals, which vary in composition from Mg_2SiO_4 (forsterite) to Fe_2SiO_4 (fayalite). On Earth, olivine makes up a large proportion of the upper mantle and is known to crystallize first from many types of basaltic magmas. Hence its detection at the surface of a planet can potentially provide important constraints on the evolution of the planetary interior. For example, the internal differentiation of most planetary bodies leads to the formation of a metal core and potentially the differentiation of the mantle, sometimes associated with the development of a magma ocean (Zerr et al., 1998; Hofmann, 1997; Labrosse, 2007). The processes that cause planetary differentiation lead to a major re-distribution of Fe within planetary bodies, for example the formation of a Fe-rich metallic core. Hence knowledge of parameters such as the Mg/Fe ratio of olivine at the surface of a planet can potentially place useful constraints on the nature and extent of differentiation of a planetary interior. During melting of the silicate portion of a planetary body, Fe is preferentially partitioned into the melt phase (Walter and Tronnes, 2004). Consequently, discovery of high Mg/Fe ratios in olivine at the surface implies a silicate mantle with low Fe content and by implication we can infer the presence of a metallic core.

Another important characteristic of olivine is that it readily alters in the presence of water into clays or iron oxides (Hoefen et al., 2003). As olivine is a mineral particularly influenced by breakdown under wet conditions, the detection of olivine on the surface of the Earth and other planets can also help us assess how long it has been at the surface and provide constraints about the climate history. For instance, the extensive detection of olivine from Mars orbit on post-Noachian surfaces indicates persistently low chemical weathering rates throughout much of Mars' history (Bandfield et al., 2000; Hoefen et al., 2003; Bibring et al., 2006).

The crystal structure of a mineral such as olivine is controlled by stoichiometric relationships, relative size of atoms (ions and cations) and the nature of molecular bonds. These characteristics can be determined by different spectroscopic techniques such as Raman spectroscopy. Raman spectroscopy is selected as a method for structural and compositional characterization of minerals in ESA's first mission of the Aurora programme, ExoMars.

In this chapter we first review the structure of olivine and then analyze how the mineral structure is affected by different chemical compositions. We then assess how these variations will influence Raman spectra and if it is viable to detect such variations using the combined Raman and Laser induced breakdown Spectrometer (RLS) instrument. In addition, a fundamental goal of this thesis is to assess if the RLS instrument is a viable instrument for operation in planetary missions, therefore experiments are carried out in our Mars atmosphere simulation chamber (MASC). Olivine spectra are taken with the RLS instrument and compared with Raman spectra determined by using a Renishaw InVia Reflex confocal

Raman microscope. Our approach is to determine olivine compositions, classify its structure using the RLS instrument based on olivine Raman vibrational modes and then examine if there are any changes when measured under Martian conditions. In addition, we will compare our Raman data to lunar and Martian samples reported by Kueble et al. (2006). This work reports olivine compositions comparable to those from Martian meteorites and the Moon. We will investigate if comparable Raman spectra are obtained and examine the relationship between Raman peak positions and the Mg value (Table 4.1) of olivines under both terrestrial and Martian conditions.

The structure of olivine

Figure 4.1 shows the general structure of olivine. Individual SiO_4 tetrahedra are linked by mainly Mg and Fe atoms, in general M atoms. Each M atom has six oxygen neighbours. Oxygen atoms are placed in sheets parallel to the (100) plane and are positioned in approximately hexagonal arrays. The orthorhombic symmetry means that Si– O tetrahedra point in alternate directions along the z and y axes (Fig. 4.1). Half of the available octahedral voids are occupied by M atoms and one-eighth of the available tetrahedral voids by Si atoms. The M atoms do not occupy a single set of equivalent lattice positions: half are placed at centres of symmetry, M1, and half on mirror planes, M2. Therefore, there are two types of octahedra in the olivine structure. The distribution of Mg^{2+} and Fe^{2+} in M1 and M2 sites records variable ordering with the larger Fe^{2+} cation commonly showing a small preference for the smaller M1 site. M1 octahedra have a shorter average M– O bond length; 2.094 and 2.161Å for forsterite and fayalite respectively (Smyth and Bish, 1988).

To quantitatively describe the tetrahedra and octahedra, we use the terms quadratic elongation and angle variance, which are both measures of lattice deformation (Fleet, 1976). Quadratic elongation is described as a unitless measure of distortion and is based on the actual bond length compared to a theoretically undistorted octahedron. Angle variance is a measure of the variance of the central angle of tetrahedra/octahedra compared to 90^o and has units of degrees squared (Smyth and Bish, 1988).

The degree of SiO_4 tetrahedral distortion is higher in forsterite (Quadratic Elongation 1.0122, Angle Variance 49.4) than in fayalite (Quadratic Elongation 1.0085, Angle Variance 36.7), which is also reflected in the length differences of the Si– O bonds in the SiO_4 tetrahedra: from 1.6139 to 1.6549 Å (difference: 0.0410) in forsterite and from 1.6248 to 1.6533 Å (difference: 0.0285) in fayalite (Smyth and Bish, 1988). As the ionic radius of Fe^{2+} (0.86Å, high spin state, Whittaker and Muntus, 1970) is bigger than that of Mg^{2+} (0.80Å), the M1 and M2 octahedra of fayalite are more comparable than those of forsterite; the volume difference between the two octahedra in fayalite is only half that of forsterite (Smyth and Bish, 1988).

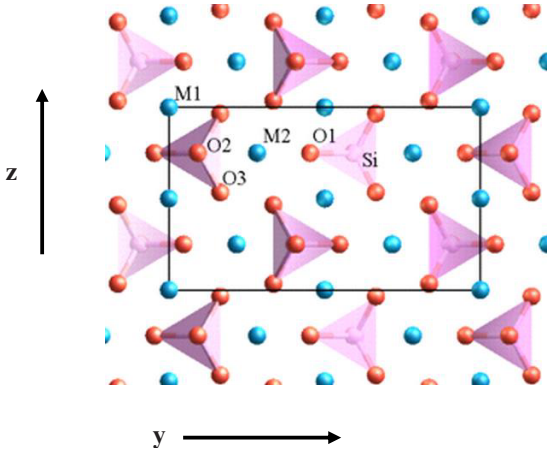

Figure 4.1. The atomic structure of olivine along the x axis is shown. Oxygen is in red, silicon in pink and magnesium/iron in blue colours. The unit cell is described by the black rectangle.

We can predict the effect of the presence of different metallic ions (Fe, Mg) on the SiO_4 tetrahedra in the olivine structure. The structural differences cause a shift of the major Raman peaks related to the stronger covalent groups in SiO_4. Here, we focus on a doublet of peaks between 815– 825 cm^{-1} (peak (a)) and 838– 857 cm^{-1} (peak (b)) and study the changes in Raman shift of the doublet based on different olivine compositions. We will examine the effect of composition on the doublet peak positions as well as relative peak heights. We also aim to assess if it is possible to determine the effect of parameters such as temperature and crystallographic orientation on the peak intensity ratio.

As mentioned above, metallic ions are bonded to oxygen. However, silicon is also in oxygen tetrahedral sites. Hence, the difference in atomic masses and bonds between Fe, Mg and oxygen affect the vibration frequencies of the strong Si– O bonds resulting in shifts in Raman peaks. Potentially, peak shifts such as peak (a) and peak (b) can be used to calculate the ratios of the cations involved. Naturally occurring olivines also have minor amounts of MnO, NiO and CaO but at generally less than 0.5 wt %. Therefore in most naturally occurring olivine, these elements are expected to have minimal effect on Raman spectra.

4.2 Sample selection

Olivine detected on Mars records a compositional range of Fo_{60} to Fo_{70} in the southwest region of Nili Fossae and Fo_{40} to Fo_{60} in the northeast region of Nili Fossae (Hoefen et al., 2003; Fo is the molar ratio and is equal to Mg/(Mg+Fe) reported in mol%). We have selected natural olivine samples with comparable compositions (olivine 1, olivine 2, olivine 3 and olivine 4) and also made use of a synthesised fayalite. Table 4.1 lists the compositions of two selected samples determined by electron microprobe analysis (EMPA) labelled olivine 1 and 2 with Fo value of 64 and 93 respectively.

Two additional olivine samples, olivine 3 and olivine 4, were also studied by EMPA. Olivine 3 and olivine 4 where obtained by mineral separation from basaltic lavas. Unfortunately, despite initial thin section studies that suggested a single olivine population both samples contained olivine with a large range of compositions and individual grains with marked zonation on a 20 μm scale. In total, Fo varied between 69 and 85. Consequently it is not viable to measure these samples with the RLS instrument as it is impractical with the current set up to analyse specific regions of an individual grain with the required spatial resolution to ensure a specific composition is measured. These samples did not provide useful information for the main goal of the study, i.e. assessing the capabilities of the RLS instrument to identify different olivine compositions under Martian conditions.

The final sample used was a pure fayalite synthesised by Dr Jellie de Vries as part of her PhD research. Table 4.2 shows the compositions of the synthesised fayalite.

Due to the small grain size (less than 15 μm) that usually characterises high pressure-temperature experimental products, we were unable to find and focus on the grains and obtain good quality Raman spectra using the RLS instrument. In contrast, the more user friendly design of the Renishaw associated with a smaller spot size (2 μm) allowed us to obtain a Raman spectrum (Fig. 4.5). EMPA determined the composition of the olivine to be Fo_{01}.

4.3 Analytical methods and data handing

Our analyses were performed with three instruments, which are described in the following sections.

4.3.1 Electron microprobe analyser

Electron microprobe analysis (EMPA) is an almost non-destructive method to determine the chemical composition of solid materials. EMPA uses a high-energy focused beam of electrons to generate X-rays that are characteristic of the elements within an unknown sample. Chemical compositions are determined by comparing the intensity of X-rays signals with those derived from standards of known composition and correcting for the effects of absorption and fluorescence in the sample. The EMPA of major element data will be compared with Raman analyses to understand how different compositions lead to different stoichiometry and how this results in changes in Raman spectra. This methodology allows the determination of the relationship between chemical composition from EPMA and spectral peak position from Raman spectra. The EMPA were collected on a JEOL JXA-8800M Superprobe with four wavelength dispersive spectrometers (WDS) at the VU University Amsterdam. Spot analyses were performed by a focused beam where the smallest practical beam diameter was used for surface analysis, in this case 1-3 μm.

	Olivine1, Fo_{64}			Olivine 2, Fo_{93}		
	Weight%	STDEV	2 σ	Weight%	STDEV	2 σ
MgO	31.79	0.44	0.23	51.27	0.18	0.10
SiO_2	37.27	0.37	0.20	40.75	0.28	0.15
FeO	31.34	0.47	0.25	6.36	0.09	0.05
CaO	0.01	0.01	0.00	0.01	0.00	0.00
Al_2O_3	0.01	0.01	0.00	0.00	0.01	0.00
MnO	0.41	0.02	0.01	0.08	0.01	0.01
TiO_2	0.01	0.01	0.01	0.01	0.01	0.00
NiO	0.14	0.01	0.01	0.35	0.01	0.01
Cr_2O_3	0.00	0.00	0.00	0.03	0.01	0.00
Total	100.98	0.40	0.21	98.86	0.33	0.18

Table 4.1. Average compositions of the olivine 1 and olivine 2 determined by EMPA.

The EMPA operating conditions were an acceleration voltage of 15 kV and the nominal beam current is about 25 nA. The counting times for the measurement of each element were 25 seconds on the peak and 12.5 seconds on the background for all oxides measured except FeO where 36 seconds were measured on the peak and 18 seconds on the background. In general minor elements are measured with longer counting times than major elements. Measurements are calibrated and standardized against well-characterized standards. In this case CaO and SiO_2 were measured in diopside. MgO in olivine, FeO in fayalite, TiO_2 in ilmenite, NiO in synthetic NiO, MnO in tephrite and Al_2O_3 in corundum.

Standard deviation (*STDEV*) and standard error (σ):

(2σ) are reported for 14, 24 and 6 analyses in samples olivine 1, olivine 2 and fayalite respectively. The true standard error of the sample mean is defined by:

$$\sigma = 2(\frac{STDEV}{\sqrt{n}}) \qquad (4.1)$$

Where *STDEV* is the standard deviation of analyses and *n* is the number of analyses of a sample. We have calculated 2σ to show the maximum error. σ (standard error) is an estimate of how close to the population mean our sample mean is likely to be, whereas standard deviation is the degree to which individuals within the sample differ from the sample mean (Gurland and Tripathi, 1971; Sokal and Rohlf, 1981).

Fayalite, Fo_{01}			
	Weight %	*STDEV*	2 σ
SiO_2	30.44	0.19	0.15
Al_2O_3	0.02	0.02	0.02
FeO	70.62	0.27	0.21
CaO	0.00	0.00	0.00
MgO	0.01	0.00	0.00
Total	101.09	0.21	0.10

Table 4.2. Average compositions of the fayalite sample determined by EMPA (De Vries, 2012).

4.3.2 Micro-Raman spectrometer

A commercial Renishaw InVia Reflex confocal Raman microscope was used for initial Raman characterisation. This commercial Raman microscope uses a 300 mW 785 nm diode laser as an excitation source in combination with a 1200 lines per mm (l/mm) grating. It has multiple optic options with 5, 20 and 50 times magnification objectives, which produce spot sizes of 20, 5 and 2 μm respectively. The spectral resolution of adjacent peaks in the system is ~ 3 cm^{-1} and accuracy of the system is about 0.1 cm^{-1}. The charge coupled detector (CCD) is cooled to -70 °C to ensure ultra-low dark noise.

4.3.3 The combined Raman and Laser induced breakdown Spectrometer (RLS) instrument

The RLS instrument uses a laser with an excitation wavelength of ~ 659 nm for Raman analysis. It weighs less than 30 g and has an output of 20 mW (For more details see chapter two). The spectral resolution is ~ 4 cm^{-1}. The RLS instrument was used to obtain Raman spectra from different olivine compositions under Martian conditions within the MASC. These experiments were also effectively a test of the ability of the RLS instrument to act as a field instrument for planetary missions. Such data are required in order to establish if the RLS instrument will be able to provide information about the processes that formed specific geological environments and hence help unravel the history of a planet in general.

4.4 Raman study of olivine

To better investigate the Raman spectra of the selected olivine samples, we first consider the vibrations of an isolated silicate tetrahedron. The isolated silicate tetrahedron is characterised by symmetric and asymmetric stretching and bending vibrations (Fig. 4.2). The symmetric stretch of the tetrahedron depends on the strength of the Si– O bond. The symmetric bending vibration, however, is controlled principally by the O– Si– O angle bending force constant. For silicate tetrahedron, peaks in the Raman spectral region between 800 and 950 cm^{-1} are formed by the vibrational modes of symmetric stretch (ν_1). The Raman peaks in the spectral region 300– 500 cm^{-1} are attributed mostly to symmetric bending vibrations (ν_2). The vibrational modes of asymmetric stretch (ν_3) produce weak Raman peaks in the spectral region 850– 1200 cm^{-1}. Finally peaks at 400– 600 cm^{-1} are attributed to asymmetric bending vibrational modes (ν_4) (Figs. 4.2 and 4.3). We expect that the effect of low temperature on the symmetric and asymmetric stretching vibration might be clearly observed as the bonds of the molecule usually become shorter at lower temperature.

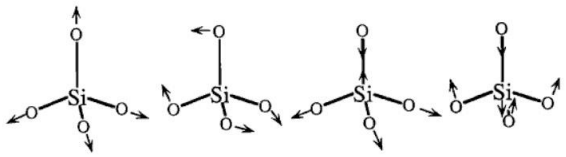

ν_1 ν_2 ν_3 ν_4

Figure 4.2. The vibration mode of an isolated silicate tetrahedron, ν_1: symmetric stretch, ν_2: symmetric bend, ν_3: asymmetric stretch, ν_4: asymmetric bend (modified from Silverstein, et al., 1981).

As mentioned previously, individual SiO_4 tetrahedra in the olivine mineral structure are connected by Mg and Fe atoms and each Mg and Fe atom has six oxygen neighbours. The olivine group forms a complete solid solution series between forsterite (Mg_2SiO_4) and fayalite (Fe_2SiO_4). The four internal SiO_4 vibration modes are supposed to be retained in the spectra but are slightly changed by the olivine crystal composition. Previous workers have demonstrated that the Raman spectrum of olivine can be practically divided into three spectral areas: < 400 cm^{-1}, 400– 700 cm^{-1} and 700– 1100 cm^{-1}(Fig 4.3; Ishii, 1978; Kuebler, et al., 2006; Chopelas, 1991).

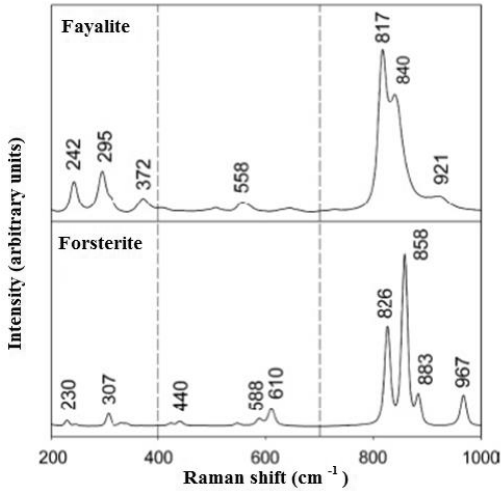

Figure 4.3. Spectra of the olivine end members: fayalite and forsterite. The three distinct areas of the spectra are divided by the dashed lines (Kuebler, et al., 2006; Note that the exact mineral compositions are not provided in the publication).

In general, peaks below 400 cm^{-1} are formed by lattice modes. Lattice modes are caused by the movements of groups of atoms in the crystalline lattice. In the olivine crystal structure, rotational and translational motions of SiO_4 tetrahedra and translational motions of octahedral cations (Mg^{2+}, Fe^{2+}) in the crystal lattice create the lattice modes (Chopelas, 1991). Peaks in the 400– 700 cm^{-1} spectral region are derived from internal bending vibrational modes of the SiO_4 ionic groups, Fig. 4.3. The peaks lower than 400 cm^{-1} and peaks in the 400– 700 cm^{-1} spectral area are usually much weaker than those in the 700– 1100 cm^{-1} region (Wang et al., 1995; 2004b). Peaks in the area of 700– 1100 cm^{-1} are attributed to the internal symmetric and asymmetric stretching modes of the SiO_4 tetrahedra. The main feature within this area is a doublet of peaks between 815– 825 cm^{-1} (peak (a)) and 838– 857 cm^{-1} (peak (b)). The positions of the doublet depend on the chemical bonds that have a higher degree of covalence. Nevertheless, because the metallic ions within olivine share an O atom with the silicate tetrahedral, the attractive force between the different ions (Fe and Mg) and difference in atomic mass can affect the vibrational frequencies of the Si– O bonds. These effects cause the shifting of the doublet peak positions when composition varies between fayalite and forsterite. They are the main reason responsible of controlling the Raman spectra of olivine in the spectrum between 700 and 1100 cm^{-1}. From Hook's law (equation 4.2), it is clear that the vibration modes are a function of the force constant of the vibration and the mass of the participating atoms:

$$\nu = \frac{1}{2\pi c}\sqrt{\frac{k_0}{\mu}} \qquad (4.2)$$

where μ is reduced mass of participating atoms (see section 2.2.4), k_o is force constant, V is vibrational frequency in wavenumber, c is speed of light. Consequently, changes in mass associated with compositional variations of olivine will produce different vibration frequencies. We should also keep in mind that at low temperature, bonds of the molecule usually become shorter. Therefore, the value of k would increase and cause possible changes in Raman peak positions.

The relationship between the Mg number (Mg/Mg+Fe) and the Raman frequency shifts of olivine has been discussed by Guyot et al., 1986; Wang et al., 1995, 2004b Kuebler et al., 2006. These studies propose correlations between the positions of the two peaks occurring between 815– 825 cm^{-1} and 838– 857 cm^{-1} in Raman spectra and the Mg value of Mg– Fe olivine. In our study we review the results of pervious work and asses the ability of the RLS instrument to identify different olivine mineral compositions under Martian conditions. We may expect an effect of temperature on strong vibration modes such as symmetric stretching vibration. Other vibration modes are weak and consequently we expect it will be hard to assess if there are small differences between terrestrial and Martian conditions.

4.5 Renishaw and RLS data of selected olivine samples

In this section, we present olivine Raman spectra obtained with: a) Renishaw Raman microscope under laboratory condition, b) RLS instrument under vacuum condition at 10 and -20 °C, c) olivine RLS spectra under CO_2 condition at -20 °C.

The Raman spectra of olivine 1 (Fo_{64}) and olivine 2 (Fo_{93}) taken with the Renishaw InVia Reflex confocal Raman microscope are presented in Fig. 4.4.

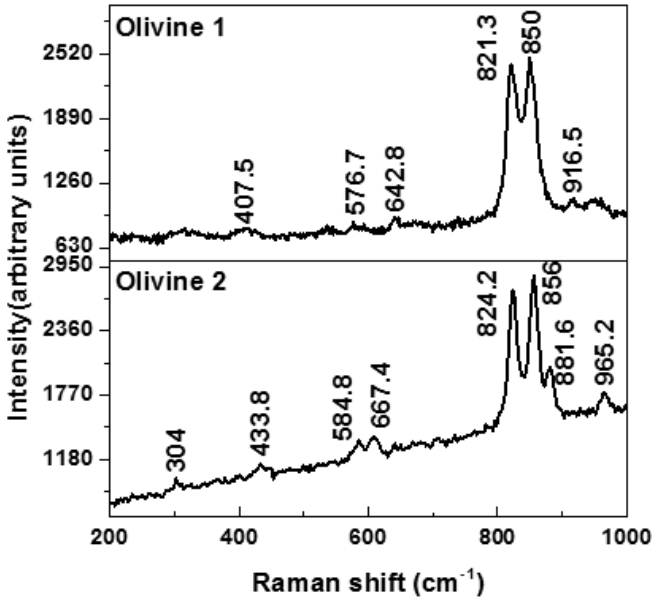

Figure 4.4. The Raman spectra of olivine 1 (Fo_{64}) and olivine 2 (Fo_{93}) taken with the Renishaw InVia Reflex confocal Raman microscope for the 200-1000 cm^{-1} region.

A Raman spectrum of fayalite (Fo_{01}) taken with the Renishaw InVia Reflex confocal Raman microscope is presented in Fig. 4.5.

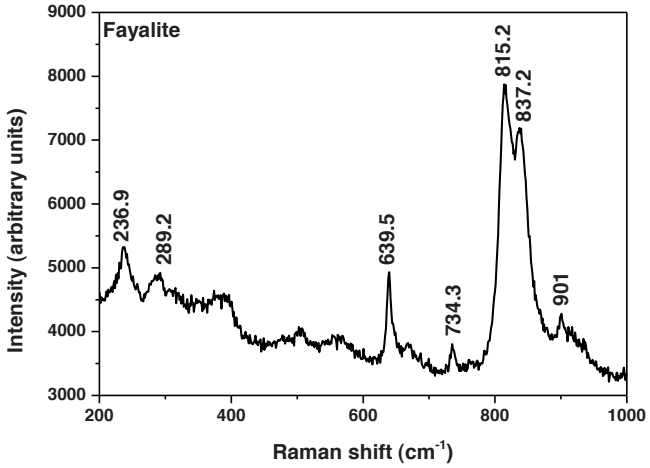

Figure 4.5. The Raman spectra of fayalite (Fo_{01}) taken with the Renishaw InVia Reflex confocal Raman microscope for the 200-1000 cm^{-1} region.

The Raman spectra obtained from 10 random grains of olivine 3 and 4 are shown in Figs. 4.6 and 4.7 respectively.

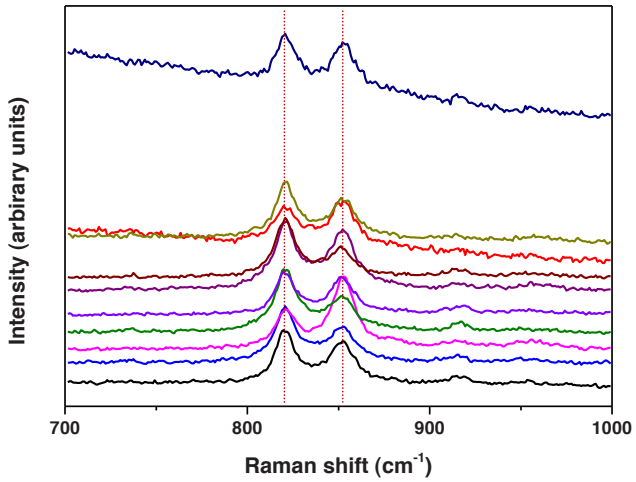

Figure 4.6. The Raman spectra obtained from 10 random grains of olivine 3 taken with the Renishaw InVia Reflex confocal Raman microscope for the 700-1000 cm^{-1} region. Spectra are vertically offset for legibility.

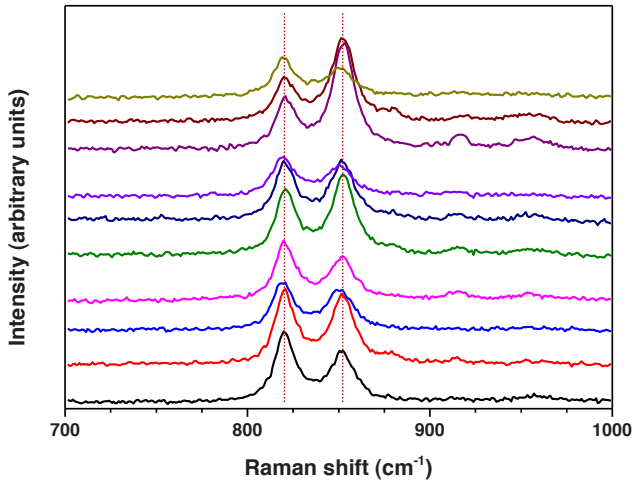

Figure 4.7. The Raman spectra obtained from 10 random grains of the olivine 4 taken with the Renishaw InVia Reflex confocal Raman microscope for the 700-1000 cm^{-1} region. Spectra are vertically offset for legibility.

The RLS Raman spectra of olivine 1 and olivine 2 are presented at Fig. 4.8. These spectra obtain under vacuum condition at 10 °C.

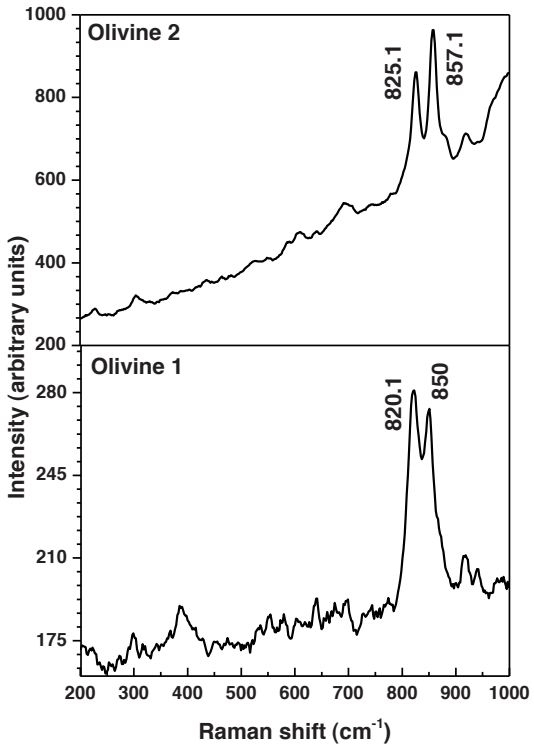

Figure 4.8. The RLS Raman spectra of olivine 1 and olivine 2 obtain under vacuum condition at 10 °C.

Raman spectra of olivine 1 and olivine 2 obtained using the RLS instrument under vacuum condition at +10 and -20 °C are present at Figs. 4.9 and 4.10.

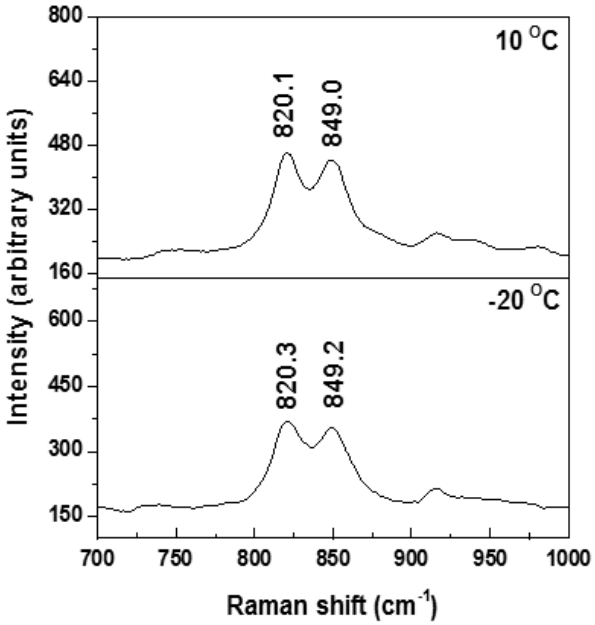

Figure 4.9. RLS Raman spectra of olivine 1 in the range 700– 1000 cm^{-1}, the measurement conditions are under vacuum condition at +10 and -20 °C.

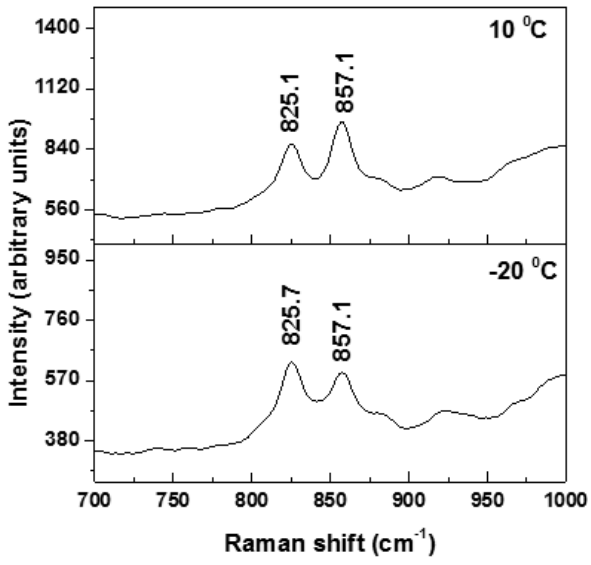

Figure 4.10. RLS Raman spectra of olivine 2 in the range 70– 1000 cm^{-1}, the measurement conditions are under vacuum condition at +10 and -20 °C.

In Figs. 4.11 and 4.12, Raman spectra of olivine 2 and olivine 1 obtained under 8 mbar CO_2 pressure at -20 °C are presented.

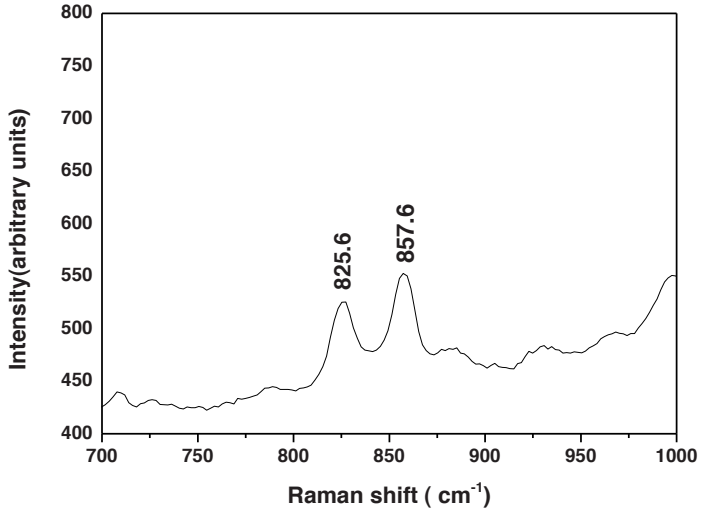

Figure 4.11. RLS Raman spectra of olivine 2 in the range 700– 1000 cm^{-1}, the measurement condition is CO_2 atmosphere with -20 °C.

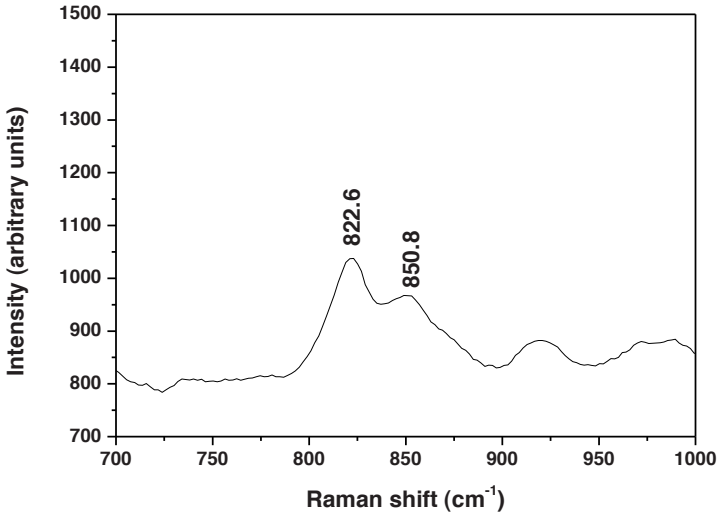

Figure 4.12. RLS Raman spectra of olivine 1 in the range 700– 1000 cm^{-1}, the measurement condition is CO_2 atmosphere with -20 °C.

4.5.1 Discussion of the Renishaw olivine data

Figure 4.4 presents the Raman spectra of olivine 1 and olivine 2 obtain with the Renishaw Raman microscope. As expected, peaks below 400 cm^{-1} and in the 400– 700 cm^{-1} spectral region are weak. These weak peaks are not often determined in multi-phase spectra from mixtures such as igneous materials (Kuebler et al., 2006). Moreover the small peak size will make effective detection under planetary conditions particularly difficult. Therefore, we focus on the 700– 1100 cm^{-1} region with stronger peak intensities, attributed to the internal symmetric and asymmetric stretching vibration modes of the SiO_4 tetrahedron. These vibration modes could be affected by temperature variations.

As we explained in the section of the Raman study of olivine, olivines with different Fo values have different Raman vibrational frequencies of Si– O bonds. According to the EMPD analyses, olivine 1 and olivine 2 have Fo value of 64 and 93. These variations are clearly resolved in the Renishaw Raman spectra with shifts in peaks (a) and peak (b) related to the change of olivine composition. The different Fo value is the major reason responsible for controlling the Raman spectra of olivine in the spectra between 700 and 1100 cm^{-1} (Fig 4.4 and Table 4.3). The observed peaks in the Raman spectrum of olivine 2 (Fo_{93}) are comparable to peaks of fosterite with Fo of 91 and 100 reported by Kuebler et al (2006).

	Fo ranging	Peak (a) cm^{-1}	Peak (b) cm^{-1}
Olivine 1	Fo_{64}	821.3	850.0
Olivine 2	Fo_{93}	824.2	856.0
Synthesised fayalite	Fo_{01}	815.2	837.2

Table 4.3. The Renishaw Raman peak positions of olivines with different Mg/(Mg + Fe) compositions.

In the Raman spectrum of the fayalite sample of Keubler et al., 2006 peak (b) appears as a shoulder of peak (a), Fig. 4.3. We establish a similar relationship in the Renishaw analysis. As an example, Raman spectrum of the synthesised fayalite, Fig. 4.5 shows peak (b) at 837.2 cm^{-1} as a shoulder of the peak (a) at 815.2 cm^{-1}. Two peaks at 639.5 and 734.3 cm^{-1} are also resolved in Renishaw Raman spectra. We considered the detection of these peaks is due to the presence of contamination (the epoxy resin) in the fayalite sample as theses peaks were not observed at pure fayalite Raman spectrum by Kuebler**.**

The variations in Raman spectra based on different Fo values for olivine 3 and 4 are shown in Figs. 4.6 and 4.7 respectively. The variations in Raman peak positions are about 2 cm^{-1} for olivine 3 and 3.5 cm^{-1} for olivine 4. These variations are significantly greater than the peak position error (~ 0.4 cm^{-1}) of the RLS instrument. Hence we can expect to detect these variations using the RLS instrument. However, due to the limitation of optical view of the sample within the MASC we could not perform measurement of specific individual grains. We encountered the same problem with the fine grained fayalite sample, which proved to be impossible to measure using the RLS instrument.

We conclude that using the Renishaw Raman microscope under laboratory condition, we could clearly resolve the different peak positions for selected olivine samples, fayalite, olivine 1 and olivine 2. Therefore, we used samples olivine 1 and 2 to assess the RLS instrument performance inside MASC under variable temperatures and atmospheric pressure.

4.5.2 Discussion of the RLS olivine data

4.5.2.1 Effect of the vacuum condition and low temperature on RLS olivine Raman spectra

In the next step of our experimental protocol samples and the RLS instrument were placed inside the MASC. Martian environmental conditions (low pressure and temperature) were applied to both the sample tray and RLS instrument. Such a study is important for further understanding how the fine structure and properties of minerals vary with physical conditions; for example possible changes in the length of atomic bonds. These data are required to assess how great is the need to characterise mineralogy under Martian conditions before the launch of ExoMars. To our knowledge only little work has yet been reported on the effect of temperature on the Raman spectra of olivine (Weber et al., 2012; Kolesov and Geiger, 2004; Chopelas, 1991) and in previous work samples were locally cooled via their sample tray or holder. In addition, there have been no specific studies based on the effect of the environment condition on the olivine spectra. Hence, we developed such studies with the RLS instrument within MASC to evaluate any possible pressure/temperature dependency of olivine Raman spectrum.

In the RLS Raman spectra of both olivine 1 and olivine 2, peaks below 700 cm^{-1} were not resolved from the background noise due to low laser power and relatively high background noise levels. In addition, these peaks are not regularly determined in mulit-phase spectra from mixtures samples (Kuebler et al., 2006). The application of the current design of the RLS instrument to planetary missions means that determination of the weak Raman peaks below 400 cm^{-1} is impractical. Peaks below 700 cm^{-1} were not the main focus of our study and we concentrated on the 700– 1100 cm^{-1} region. The most characteristic olivine peaks with the strongest intensity appear in this spectral region.

In Fig. 4.8, we present RLS Raman spectra of olivine 1 and olivine 2 obtained under vacuum (10^{-5} mbar) at 10 °C. The reported RLS spectra focus on the positions of the olivine doublet peak in the 700– 1000 cm^{-1} region. Compositional variations in the olivine 1 and olivine 2 (Fo_{64} and Fo_{93}) result in clear shifts in the wavelengths of the doublet peaks between the two olivine samples. The RLS Raman spectrum of olivine 2 (Fo_{93}) has distinct peaks at 825.1 cm^{-1} and 857.1 cm^{-1}. The maximum intensity occurred at the second of these two peaks. In the RLS Raman spectra of olivine 1 (Fo_{64}), the doublet is less well resolved than of olivine 2 (Fo_{93}) and the peak near 850.0 cm^{-1} appears as a shoulder of the peak near 820.1 cm^{-1}.

In general, the double peaks in fayalite Raman spectra are closer together (lower resolution) due to the less distorted SiO_4 tetrahedra and this leads to a less complex Raman spectra (Kuebler et al., 2006). The lesser separation of the doublet peaks in olivine 1 is because of the

less distorted SiO_4 tetrahedra and greater similarity of the M1 and M2 octahedra in the olivine 1 mineral structure compared to olivine 2 structure.

As a test that the samples chosen for study were representative of potential lunar and Martian samples, we compare the RLS Raman data with the Raman data of Martian meteorite EETA 79001.530 and Twin Sister (eight lunar, Martian and terrestrial olivine samples from Kueble et al., (2006)). Olivine 1 from this study has Fo value (64) close to EETA 79001.530 (Fo_{62}) and olivine 2 has Fo value (93) as Twin Sister (Fo_{92}). We confirmed that we obtain comparable Raman peak positions for olivine 2 and EETA 79001.530 and olivine 1 and the Twin Sister samples (Table 4.4).

sample	Fo	Peak (a) (cm^{-1})	Peak (b) (cm^{-1})
Olivine 2/Twin Sister	Fo_{93}/Fo_{91}	825/823	857/855
Olivine 1/EETA 79001.530	Fo_{64}/Fo_{62}	820/820	850/849

Table 4.4. Comparison between Raman peaks from Kueble et al., 2006 and RLS Raman peaks form olivine 1 and olivine 2 under vacuum (10^{-5} mbar) at 10 °C.

In the next part of our study we examine the influence of temperature on RLS Raman spectra under conditions expected to be used for the ExoMars mission. Our study is a practical approach designed not to resolve potential marked variations in Raman spectra at extreme temperatures but as a test of the effects likely to be encountered by Raman analysis by the ExoMars rover. ExoMars experiments are expected to be performed inside the rover at temperatures in the range 10 to -30 °C.

The data obtained in our experiments at temperatures between 10 and to -20 °C are presented in Table 4.5 and Figs 4.9 and 4.10. The position of peak (a) near 825 and 820 cm^{-1} in olivine 2 and olivine 1 and peak (b) near 857 and 849 cm^{-1} in olivine 2 and olivine 1 show no resolvable change with temperature; i.e. within the ~ 0.4 cm^{-1} error of the RLS instrument. The work of Kolesov (2004), similarly reported that there is no shift in the two peaks of the fayalite sample at temperatures between -40 to -268 °C.

In chapter two (section 2.2.2), it was discussed that the intensities of specific peaks depends on the polarizability of the molecule in the mineral, the intensity of the laser excitation source and the concentration of the Raman active group in the mineral structure. Therefore, we initially considered undertaking a rigorous assessment if it was possible to use intensity ratios of the different Raman peaks to establish if such parameters also proved to be a characteristic feature of Raman spectra of olivine in terms of composition, crystallographic orientation and temperature.

Most minerals have different optical properties depending on the cyrstallographic orientation. Previous work by Ishii (1978) and Chopelas (1991) established that this is the case for the orthorhombic olivine mineral group. Consequently the intensity of Raman peaks is known to change depending on the crystallographic orientation of the mineral.

Kolesov (2004) also reported a change of the relative intensity of fayalite Raman peaks at low temperature (-40 to -268 °C). The change of intensity might be a result from Fe in olivine, by which magnetic interactions can take place. In our measurements we also observe the effect of the Fe in the structure of olivine 1 at lower temperature with a decrease the intensity of the peak at 857.1 cm^{-1} in olivine 2. For example, in olivine 2, the intensity ratio of peak (a)/peak (b) under vacuum at 10 °C is 0.89. However, this intensity ratio at -20 °C is about 1.02.

The data presented above establishes that there are distinct variations in the intensity ratios between Raman peaks. Unfortunately, initial work with the RLS instrument immediately proved that it is impractical to determine the crystallographic orientation of each mineral under study in a context that mimics field conditions i.e., as the RLS instrument would be used upon Mars. More importantly in respect of the planned experimentation, the laser excitation wavelength in the RLS instrument (and the power output 20 mW) was unstable making it impossible to consistently produce repeatable data. Hence, we were unable to make a quantitative assessment of if we could use the intensity ratio of Raman peaks to study, for example, olivine composition or crystallographic orientation. The latter is probably of limited use in most geological environments but the ability, for example, to determine if minerals have a preferred orientation could provide valuable information about geological or bio-geochemical processes.

From this work we are only able to conclude that the intensity of Raman peaks in natural minerals is variable as is the intensity ratio between peaks. Further work will be required with a stable instrument to assess if peak intensity ratios can be used to help distinguish different olivine compositions and/or crystallographic orientation.

We conclude that for olivine there is no resolvable change (based on the temperature) in peak positions under the analytical conditions operable inside the ExoMars Rover. Hence, these data establish that the potential temperature induced variation in peak position discussed previously is not relevant over the range studied in this work (+10 to -20 °C). Moreover, the study of Raman peak couplet is a viable technique for determining olivine composition on Mars using the RLS instrument.

	Olivine 2		Olivine 1	
Vibration modes (cm^{-1})	10 °C	-20 °C	10 °C	-20 °C
Peak (a)	825.1	825.7	820.1	820.3
Peak (b)	857.1	857.1	849.0	849.2

Table 4.5. RLS Raman peaks of olivine 1 and olivine 2 at 10 and -20 °C.

4.5.2.2 Effect of 8 mbar CO_2 pressure at low temperature on olivine Raman spectra

In Figs. 4.11 and 4.12, the Raman spectra are reported for olivine 1 and olivine 2 obtained at -20 °C in an atmosphere of 8 mbar CO_2. The identification of peak (a) and peak (b) in the olivine Raman spectra were possible (Table 4.6). In olivine 2 peak (a) and peak (b) are recorded with the Raman shifts of 825.6 and 857.6 cm^{-1}. For olivine 1 Raman shifts are 822.6 and 850.8 cm^{-1}. The positions of the peaks reported in Table 4.6 for olivine 2 and olivine 1 under CO_2 atmosphere conditions are within ~ 0.5 and 2 cm^{-1} those obtained under vacuum conditions. Since the peaks were not well resolved the exact peak position could not be determined.

We estimate that the error in peak identification for olivine 1 (~ 2 cm^{-1}) under Martian conditions was due to none-resolved peaks. Hence we cannot confidently detect any shift in wavenumber in the olivine 1 spectra. The intensity ratios of the Raman spectra are comparable to spectra obtained under vacuum conditions.

	Olivine 2		Olivine 1	
Vibration modes (cm^{-1})	10^{-5} mbar Vacuum condition	8 mbar CO_2 pressure	10^{-5} mbar Vacuum condition	8 mbar CO_2 pressure
Peak (a)	825.7	825.6	820.3	822.6
Peak (b)	857.1	857.6	849.2	850.8

Table 4.6. RLS Raman peaks for olivine 1 and 2 under vacuum (10^{-5} mbar) and at 8 mbar CO_2 condition; at -20 °C in both cases.

4.6 Conclusion

With the RLS instrument under vacuum/CO_2 condition at 10 and -20 °C, the doublet peaks in the 820 to 860 cm^{-1} range were identifiable and the intensity of these peaks mean that olivine identification under Martian conditions is clearly possible. However, in the context of application of the RLS instrument under planetary conditions it must be noted that the determination of some lattice vibration modes that produce weak Raman peaks was not possible. To detect weak peaks, we need to increase the laser power and/or operate the CCD at lower temperature (-70 °C) to increase the signal to noise ratio.

Olivine produces Raman modes in the 200 to 1000 cm^{-1} range. Comparison of the frequencies of the various mode categories indicates that the doublet peak in the 820 to 860 cm^{-1} range is most sensitive to compositional variation. These data are similar to those found for the Raman spectra reported in the work of Kuebler, et al., (2006). These data suggest that not only can accurate spectral data yield good estimates of determining different type of olivine

but the opposite may also be true, i.e., that accurate Fo calculation can be used to estimate spectral properties.

We should keep in mind that the identification of the doublet peaks depends on the resolution of the RLS instrument (4 cm^{-1}). Further study is needed with numerous (> 10) olivine compositions (Fo_{01}– Fo_{100}) to fully determine the resolution that can be achieved by the RLS instrument.

Further study at the lower temperature is needed to evaluate any effect of low temperature on the peak (a) and peak (b) in olivine Raman spectrum that may be required for the application of Raman studies on atmosphere free planetary bodies where temperatures will be significantly lower than on Mars or in the case of Mercury potentially higher than on Mars. In general, the effect of very low temperatures on mineral structure (lower that -95 °C) is expected to result in changes of Raman peak position, peak widths, peak intensities and appearance of new peaks (Sobron and Wang, 2011).

4.7 References

Bandfield, J. L., V. E. Hamilton and P. R. Christensen, (2000), A global view of Martian surface compositions from MGS-TES: Science, Vol. 287, p.1626-1630.

Bibring et al., (2006), Global Mineralogical and Aqueous Mars History Derived from OMEGA/Mars Express Data, Science 312 (5772), p. 400–404.

De Vries, J. (2012), Lunar Evolution; a combined numerical modelling and HPT experimental study, PhD thesis, Utrecht University, Netherlands.

Chopelas, A. (1991), Single crystal Raman spectra of forsterite, fayalite, and monticellite. Am Mineral Vol. 76, p. 1101–1109.

Fleet, M. E., (1976), Distortion parameters for coordination polyhedra: Mineralog. Mag., U 40, p. 531-533.

Gurland, J, R. C. Tripathi, (1971), A simple approximation for unbiased estimation of the standard deviation". American Statistician (American Statistical Association) 25 (4), p. 30–32.doi:10.2307/2682923. JSTOR 2682923.

Guyot, F. et al., (1986), Comparison of the Raman microprobe spectra of $(Mg,Fe)_2$ SiO_4 and Mg_2GeO_4 with olivine and spinel structures. Phys. Chem. Mineral. Vol. 13, p. 91–95.

Hoefen, T. M. et al., (2003), Discovery of olivine in the Nili Fossae region of Mars. Science. Vol. 302, p. 627-630.

Hofmann, A. W. (1997), Chemical differentiation of the Earth: The relationship between mantle, continental crust and oceanic crust. Earth Planet. Sci. Lett. 90, p. 297-314.

Ishii. K., (1978), Lattice dynamics of forsterite. Am. Mineral. 63, p. 1198–1208.

Kolesov, B. A., C. A. Geiger, (2004), A temperature-dependent single-crystal Raman spectroscopic study of fayalite: evidence for phono-magnetic excitation coupling, vol. 31, pp. 155-161.

Kuebler, K. E. et al., (2006), Extracting olivine (Fo–Fa) compositions from Raman spectral peak positions. Geochimica et Cosmochimica Acta. Vol. 70, p. 6201-6222.

Labrosse, S., J. W. Hernlund and N. Coltice, (2007), A crystallizing dense magma ocean at the base of the Earth's mantle. Nature 450, p. 866-890.

Smyth, J. R. and D. L. Bish, (1988), Crystal structures and cation sites of the rock-forming minerals, Allen and Unwin, Boston, Massachusetts, pp. 332.

Sobron P., A. Wang, (2011), A planetary environment and analysis chamber for combined in-situ spectroscopic measurements on selected materials under planetary relevant environments, J. Raman Spectroscopy, doi:10.1002/jrs.3017.

Sokal, R. R. and F. J. Rohlf, (1981), Biometry: Principles and Practice of Statistics in Biological Research, 2nd ed. ISBN 0-7167-1254-7 , p. 53.

Silverstein, R. M., G. C. Bassler, T. C. Morrill, (1981), Spectrometric Identification of Organic Compounds. 7th ed., John Wiley & Sons Inc., USA, p. 95-98.

Walter, M. J., R. G. Tronnes, (2004), Early Earth differentiation Earth and Planetary Science Letters, 225, p. 253–269.

Wang, A., B. L. Jolliff, L. A. Haskin, (1995), Raman spectroscopy as a method for mineral identification on lunar robotic exploration missions. Journal of Geophys, Res. Vol. 100, p. 21189–21199.

Wang, A., K. Kuebler, B. L. Jolliff, L. A. Haskin, (2004b), Mineralogy of a Martian meteorite as determined by Raman spectroscopy. J. Raman Spectrosc. Vol, 35, p. 504–514.

Whittaker, E. J. W and R. Muntus, (1970), Ionic radii for use in geochemistry Geothim Cosmochim Acta, Vol. 45, p. 945-956.

Weber, I. et al., (2012), Raman spectra of olivine measured in different planetary Environments, European Planetary Science Congress (EPSC), Vol. 7, p. 156.

Zerr, A., A. Diegeler and R. Boehler, (1998), Solidus of Earth's deep mantle. Science Vol. 281, p. 243-246.